Interface Focus

rsfs.royalsocietypublishing.org

Research

Cite this article: Tonazzini I, Pellegrini M, Pellegrino M, Cecchini M. 2014 Interaction of leech neurons with topographical gratings: comparison with rodent and human neuronal lines and primary cells. *Interface Focus* **4**: 20130047.
http://dx.doi.org/10.1098/rsfs.2013.0047

One contribution of 10 to a Theme Issue 'Nano-engineered bioactive interfaces'.

Subject Areas:
nanotechnology, biomedical engineering, biomaterials

Keywords:
gratings, neurite, contact guidance, mechanotransduction, filopodia, growth cones

Author for correspondence:
Ilaria Tonazzini
e-mail: ilaria.tonazzini@sns.it

Electronic supplementary material is available at http://dx.doi.org/10.1098/rsfs.2013.0047 or via http://rsfs.royalsocietypublishing.org.

Royal Society Publishing

Interaction of leech neurons with topographical gratings: comparison with rodent and human neuronal lines and primary cells

Ilaria Tonazzini[1], Monica Pellegrini[2], Mario Pellegrino[3] and Marco Cecchini[1]

[1]NEST, Scuola Normale Superiore and Istituto Nanoscienze-CNR, Piazza San Silvestro 12, Pisa 56127, Italy
[2]Scuola Normale Superiore, Piazza dei Cavalieri 7, Pisa 56126, Italy
[3]Dipartimento di Ricerca Traslazionale e Delle Nuove Tecnologie in Medicina e Chirurgia, Università di Pisa, Via S. Zeno 31, 56127 Pisa, Italy

Controlling and improving neuronal cell migration and neurite outgrowth are critical elements of tissue engineering applications and development of artificial neuronal interfaces. To this end, a promising approach exploits nano/microstructured surfaces, which have been demonstrated to be capable of tuning neuronal differentiation, polarity, migration and neurite orientation. Here, we investigate the neurite contact guidance of leech neurons on plastic gratings (GRs; anisotropic topographies composed of alternating lines of grooves and ridges). By high-resolution microscopy, we quantitatively evaluate the changes in tubulin cytoskeleton organization and cell morphology and in the neurite and growth cone development. The topography-reading process of leech neurons on GRs is mediated by filopodia and is more responsive to 4-μm-period GRs than to smaller period GRs. Leech neuron behaviour on GRs is finally compared and validated with several other neuronal cells, from murine differentiated embryonic stem cells and primary hippocampal neurons to differentiated human neuroblastoma cells.

1. Introduction

Cell contact interaction with extracellular domains is important for many physiological processes *in vivo* (e.g. during embryogenesis, tissue formation or regeneration) [1–3] and can be exploited to manipulate cell morpho-functional responses *in vitro* [4–6].

In the central nervous system (CNS), the contact sensing combines with a complex dynamical signalling pattern that is integrated by cells to establish the final neuronal polarity and to form a functional network of neuronal connections [7–9]. Extracellular nano/microtopography signals are locally retrieved through a complex phenomenon called contact guidance and can drive many neuronal activities, such as differentiation, polarization, neurite pathfinding, nucleokinesis and the final CNS wiring [10–16]. These processes are tightly regulated and involve coordinated interactions between microtubules and the actin cytoskeleton [16,17] as well as the establishment and maturation of focal adhesions (FAs) [18]. In particular, growth cones (GCs)—dynamic structures rich in actin filaments at the tips of neurites—move by probing environmental cues by filopodia [13,19,20] and integrating multiple sources of physico-chemical information. Recently, it has been shown that several neuronal subpopulations, or even the same neuronal types but at a different maturation stage, can read and respond differently to the same guidance cue during migration and differentiation [21,22].

Owing to the recent developments in micro/nanoengineering techniques, the processes that control neuronal guidance and differentiation can now be directly investigated using nano/microtextured substrates [23–28]. In particular, in the last few years nanogratings—anisotropic topographies composed of alternating lines of grooves and ridges with submicrometre lateral dimensions—have been intensively investigated and have emerged as one of

the most effective systems for inducing neuronal alignment via pure cell mechanotransduction. In previous studies, we showed that the interaction of nerve growth factor (NGF)-differentiating PC12 cells with these substrates promotes bipolarity and alignment to the substrate topography by interfering with FA establishment and maturation [29–31]. The ability to direct neurite growth depends on both the dimensions of the underlying patterned substrate and, very importantly, on the neuronal cell type [31–33].

Invertebrates, for example leeches, have proved to be useful models for studying neuronal dynamics [34–36]. The simple nervous system and cellular accessibility, together with the large size and the single neuron identifiability *in vivo* and *in vitro*, are some of the invertebrate advantages that allowed us to improve the knowledge about evolutionarily conserved neuronal mechanisms [37]. Moreover, it is worth mentioning the contribution of pioneering experimental studies performed on invertebrates that permitted the identification of the basic mechanisms of neuronal functions [38–40]. Both cell body and GC membranes of leech neurons express mechanosensitive cation channels with pharmacological features similar to those found in vertebrate cells [41]. For example, blocking these channels affects neurite outgrowth in culture [42], an issue confirmed later in vertebrate neurons [43]. Interaction of isolated leech neurons with patterned substrates was only recently proposed *in vitro* to address the influence of micrometre-sized lines with heights of 10–150 nm [44,45] on neurite outgrowth.

Here, we investigate neurite contact guidance of leech neurons on topographical gratings (GRs) of varying periodicity. By using high-resolution fluorescence microscopy on immunostained cells, we quantitatively evaluated the changes in tubulin cytoskeleton organization and cell morphology, and the neurite network and filopodia development induced by mechanotransduction. Leech neuron contact guidance was finally compared and validated with several other neuronal cells, from differentiated human neuroblastoma cells to primary murine hippocampal neurons.

2. Material and methods

2.1. Substrate fabrication

GRs were fabricated by thermal nanoimprint lithography on copolymer 2-norbornene ethylene (cyclic olefin copolymer (COC)) foils (IBIDI, Martinsried, Germany). COC was chosen because of its well-documented biocompatibility and optimal optical properties for high-resolution fluorescence microscopy. Nanoimprint lithography is based on the combination of pressure and heat, which aids the transfer of the chosen pattern from a rigid mould to thermoplastic materials. Moulds were fabricated by electron beam lithography and dry etching techniques, as reported in [46]. COC foils were imprinted using an Obducat Nanoimprint 24 system (Obducat, Lund, Sweden). After cleaning with nitrogen flow, the substrates were placed on top of the silicon moulds and softened by raising the temperature up to 150°C. A pressure of 50 bar was then applied for 5 min before cooling down to 70°C, i.e. below the glass transition temperature of the copolymer (Tg = 134°C). Finally, the pressure was released and the mould was detached from the substrate with a scalpel. The imprinted substrates were quality checked by optical microscopy and attached to the bottom of hollow 35 mm Petri dishes by using silicone glue (RS Components RS692-524). Before cell culturing, the samples were sterilized by treatment with ethanol, and then rinsed with phosphate-buffered saline (PBS) twice and with H_2O_{mQ} once. The GRs had linewidth

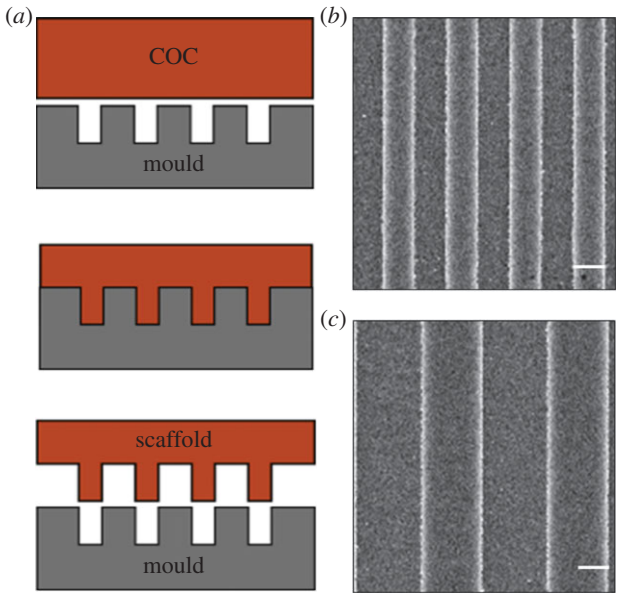

Figure 1. Substrates with surface GRs. (*a*) Schematic representation of the fabrication process: the silicon moulds are fabricated by electron beam lithography (EBL) and reactive-ion etching (RIE); thermal nanoimprint lithography is exploited to transfer the pattern from the moulds to thermoplastic materials as the copolymer 2-norbornene ethylene (COC). (*b,c*) Scanning electron microscopy images of COC GRs: T2 (*b*) and T4 (*c*); scale bars, 1 µm. (Online version in colour.)

of 1 µm (T2) and 2 µm (T4) (ridge width = groove width; figure 1) and groove depth was 350 nm for all the substrates. Flat COC surfaces (named FLAT) were used as a control.

2.2. Leech neuronal cell culture and immunostaining

Adult specimens of *Hirudo medicinalis* L. were obtained from a commercial supplier (Ricarimpex, Eysines, France) and prepared as previously reported [36]. Briefly, segmental ganglia were removed from the CNS of anaesthetized animals (chlorobutanol 0.15%; Sigma, Milan, Italy). Neuronal cell bodies of the ventral lateral packet were collected and plated onto concanavalin A (Sigma)-coated COC substrates [47]. Cells were maintained in Leibovitz-15 medium supplemented with 0.6% glucose, 2% fetal calf serum and gentamicin 200 µM (Sigma), at 20°C for 2–4 days. Leech neurons were fixed for 10 min with 4% formaldehyde/4% sucrose in PBS at room temperature and processed as previously reported [48]. After fixation, the cells were washed in PBS at room temperature, and then incubated with mouse anti-tubulin-α (Sigma t5168; 1 : 500) primary antibody in GDB solution (0.2% bovine serum albumin, 0.8 M NaCl, 0.5% Triton X-100, 30 mM phosphate buffer, pH 7.4) containing phalloidin-Alexa647 (Invitrogen A22287; 1 : 20), overnight at 4°C. Samples were then washed three times in PBS at room temperature and incubated with Alexa488-conjugated secondary antibody (Invitrogen, 1 : 100) in GDB solution for 2 h at room temperature, and washed three times in PBS. As previously reported, other neuronal cell models were processed on GRs as follows. PC12 cells were cultured for 4 days with NGF 100 ng ml^{-1} [31] and immunostained for tubulin-βIII (Sigma T2200; 1 : 50). F11 hybridoma cells, a fusion of a mouse dorsal root ganglion and a rat neuroblastoma, were differentiated for 4 days with forskolin 10 µM in 1% fetal bovine serum (FBS) medium [24] and immunostained for vinculin (Sigma; monoclonal, 1 : 100). SH-SY5Y cells (ATCC, CRL-2266) were seeded on collagen type I (50 ng ml^{-1})-coated GRs and differentiated with retinoic acid 10 µM and brain-derived neurotrophic factor (BDNF) 50 ng ml^{-1} in 1% FBS medium for a total of 10 days and immunostained for

tubulin-βIII (Abcam 78078; 1 : 200). Mouse (strain UBE3/129Sv) hippocampal neurons were set up from E17 embryos [48], grown and immunostained on D14 *in vitro* for tubulin-α (Sigma t5168) [49]. Mouse embryonic stem cells were seeded (1500 cells cm^{-2}) on 0.1% gelatin-coated GRs and differentiated in neurons [50] and on D14 immunostained for tubulin-βIII. All samples were incubated in GDB solution containing primary antibodies and phalloidin-Alexa647 (1 : 20–1 : 50), as for leech neurons. Samples were mounted using Vectashield mounting medium with 4′,6-diamidino-2-phenylindole (DAPI) (Vector Laboratories).

2.3. Fluorescence microscopy

For quantification, confocal images were acquired using a laser scanning confocal microscope TCS SP2 (Leica Microsystems, Wetzlar, Germany) with a 40× or 63× oil objective, at 1024 × 1024 pixel resolution. Each confocal image was a *z*-series (stack depth was 4–10 μm; steps = 0.5 μm), each averaged three times, and was chosen to cover the entire region of interest from top to bottom. The resulting *z*-stack was processed by ImageJ software (National Institutes of Health, Bethesda, MD, USA) into a single image using 'z-project' and 'max intensity' options.

2.4. Image and statistical analysis

Neuronal cytoskeleton polarization was quantified by analysing the tubulin fluorescence signal of each cell with the directionality tool of the software Fiji (http://fiji.sc/Fiji), as in [49]. This plugin returns a directionality histogram by exploiting image fast Fourier transform (FFT) algorithms: isotropic images generate a flat histogram, whereas oriented images are expected to give a histogram peaked at the orientation angle. These histograms are finally fitted by Gaussian curves that return two parameters, dispersion and directionality (the standard deviation and the centre of the Gaussian curve, respectively). Cell alignment (named *aligned tubulin signal*) was reported as the percentage of the FFT signal within ±16° from the GR direction, as in [49].

Leech neurites were semi-automatically segmented (from the point of origin on the cell body to the tip of the neurite GC) from the tubulin-stained images using NeuronJ, a plugin of ImageJ. Neurites were segmented according to their branching [51]. A file containing the tracks was exported and loaded into Matlab (MathWorks) to calculate the neuritic segment length (the distance of the traced path) and alignment (measured by approximating the segment as a straight line from the initial point to the endpoint and taking the angle of this line with respect to the GR orientation) [27]. Segments with length less than 1 μm were excluded from this analysis. The GR direction was measured as an angle by the ImageJ angle tool; for FLAT substrates, a random reference angle was chosen. To quantify the alignment of the neuronal network, the neurites were considered 'aligned' if the angle with respect to the GR direction was less than or equal to 15° [30].

Filopodia at the GCs were traced on actin-stained high-resolution images and measured (for length and alignment angle) as described earlier for the neurite segment analysis. Filopodia were traced from the emerging point of the GC to their end. Similar to [19], the filopodium actin content was quantified by measuring the average intensity of the fluorescent F-actin: data were reported as the ratio of the fluorescence intensity from aligned filopodia (alignment angle less than or equal to 15°) over the fluorescence intensity from the misaligned ones (alignment angle greater than or equal to 45° versus GR).

Data are reported as average value ± standard deviation (mean ± s.d.); in total, 40 leech neurons and 46 GCs were quantified. Three independent experiments were carried out for each substrate showing consistent results. Data were statistically analysed by the GraphPad PRISM 5.00 program (GraphPad Software, San Diego, CA, USA). One-way ANOVA Tukey's multiple comparison test or Kruskal–Wallis test (for non-parametric data) analyses were used. Statistical significance refers to results where $p < 0.05$ was obtained.

3. Results

GRs, biocompatible nanostructured scaffolds with alternating lines of micrometre ridges and grooves, were fabricated by thermal nanoimprint lithography on COC foils (figure 1*a*). Their optical properties and thickness (0.18 mm) allow high-resolution imaging of living cells [29]. The nanoimprinting protocol yielded reproducible GRs, with 50% duty cycle (i.e. ridge width = groove width), 350 nm depth and linewidth of 1 μm (T2) and 2 μm (T4) (figure 1*b*,*c*). Importantly, surface wettability was not affected by the imprinting procedure or by the presence of GRs [46]. GRs allow breaking of the symmetry of the cell-contacting surface, transferring a full directional mechanical impulse to the cells.

Leech neurons were dissociated and cultured on T2, T4 and FLAT substrates (chosen as the isotropic control surface) for 4 days. On FLAT surfaces, neurites grew randomly oriented, without showing any preferential outgrowth spatial bias (figure 2*a*). On GRs, neurons were clearly polarized and aligned along the GR lines. This effect was more pronounced on T4 (figure 2*b*,*c*) than on T2. GCs at the tip of neurites presented actin-rich filopodia, the cellular structures assigned for the surrounding sensing. High-resolution images of neurite tips with GCs give indications on the dynamical processes by which neurites can retrieve contact guidance information and explore the substrate topography. On T2, neurites appeared thinner and more segmented than on T4 but with tips and GCs aligned to the topography (figure 2*e*). On T4, neurites bundled parallel to the GRs and exhibited GCs with filopodia following the GR lines (figure 2*f*).

In order to quantify the degree of neuronal alignment, the tubulin signal was first analysed, as described in §2.4. We measured the cell tubulin signal by image FFT algorithms. As shown in figure 3*a*, the aligned tubulin signal was 33.3 ± 7.6% on T2 and 52.1 ± 15% on T4, while on FLAT it was 19.9 ± 3.5%. These data demonstrate that leech neurons can develop following the GR directional signal ($p < 0.01$ FLAT versus T2 and $p < 0.001$ FLAT versus T4; one-way ANOVA, Tukey's test). This effect was more pronounced for cells on T4 than on T2 ($p < 0.001$ T4 versus T2; one-way ANOVA, Tukey's test).

The neuritic arborization was then quantitatively characterized. Briefly, neurites were divided in straight segments and their lengths and orientations were measured. Both T2 and T4 induced neurite network alignment to the substrate topography. Specifically, on T2 and T4 61.2 ± 10.6% and 81.6 ± 10.8% of the total neuritic length derived from aligned segments (i.e. forming an angle less than or equal to 15° with respect to the GR lines), respectively. On FLAT this percentage, which was calculated with respect to a random direction, reduced to 17.9 ± 2.5% ($p < 0.001$ FLAT versus T2 and T4; one-way ANOVA, Tukey's test; figure 3*b*). The neurite alignment was better on T4 than on T2 ($p < 0.05$ T4 versus T2; one-way ANOVA, Tukey's test). The better performance of T4 was also confirmed by the measure of the average alignment angle of neurite segments, which was 14.6 ± 17.3° for T4 and 25.6 ± 23.8° for T2. As expected, the neurite segments on FLAT did not show a biased angular distribution ($p < 0.001$ FLAT versus T2 and T4; $p < 0.001$ T4 versus T2; one-way ANOVA, Kruskal–Wallis test; figure 3*c*).

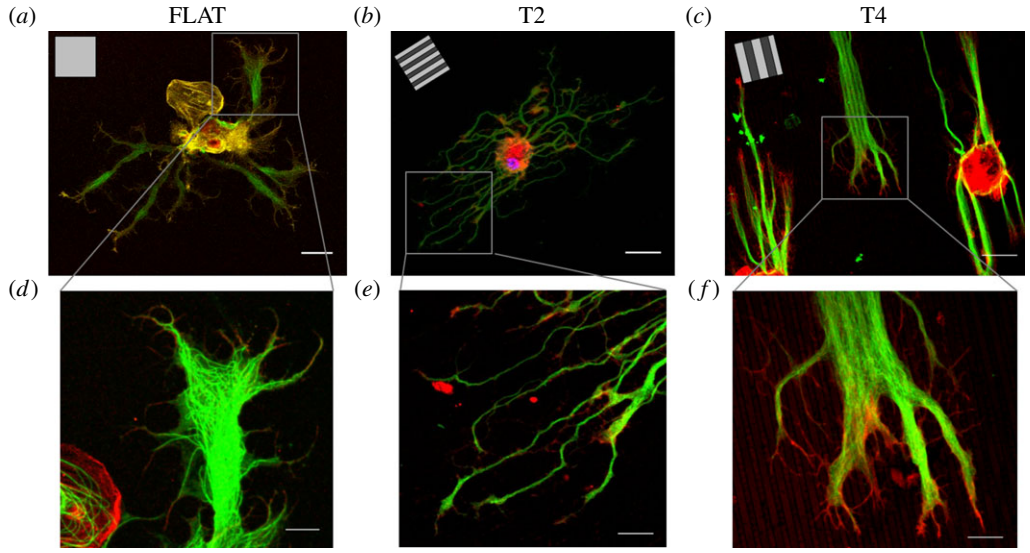

Figure 2. Confocal images of leech neurons cultured on FLAT, T2 and T4. (*a–c*) Leech neurons were grown on FLAT (*a*), T2 (*b*) and T4 (*c*) substrates and immunostained for tubulin-α (green) and actin (red); scale bars, 30 µm; inset, GR pattern direction. (*d–f*) Details of leech GCs developing on FLAT (*d*), T2 (*e*) and T4 (*f*); scale bars, 10 µm.

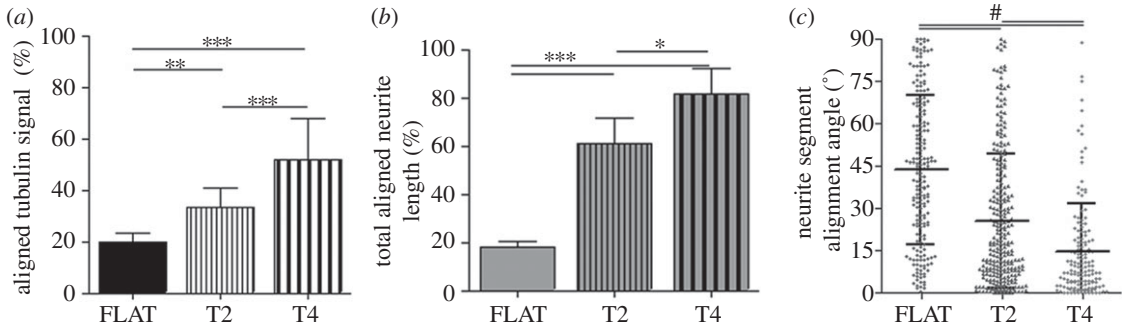

Figure 3. Leech neurons were grown on T2, T4 and FLAT substrates for 4 days. (*a*) Tubulin cytoskeleton directionality analysis. The FFT tubulin fluorescence signal aligned to the GR (within 16°) is reported for different GRs. (*b*) Leech neurites were traced and the total length of the neurite network aligned to the GR (alignment angle less than or equal to 15°) is reported as the percentage over the total neurite network length for the different substrates. (*c*) Mean alignment angle of neurite segments for the different substrates. (*a,b*) *$p < 0.05$, **$p < 0.01$, ***$p < 0.001$, one-way ANOVA, Tukey's test; (*c*) #$p < 0.001$, one-way ANOVA, Kruskal–Wallis test. Data are reported as mean ± s.d.

In order to better describe the cellular mechanisms allowing topographical guidance and consequent neuronal polarization on GRs, we investigated filopodium development at the GCs. Filopodia were traced and quantified on high-resolution confocal images of phalloidin-stained neurite tips on T2, T4 and FLAT substrates (figure 4). On FLAT, GCs (figure 4*a*) were more spread and showed a high density of randomly oriented filopodia (9.6 ± 1.7 filopodia/GC), while on T2 and T4 the GCs (figure 4*b*,*c*) were streamlined with fewer filopodia (7.1 ± 3.4 and 6.0 ± 0.8 filopodia/GC, respectively) mainly oriented along GR tracks ($p < 0.1$ FLAT versus T2 and $p < 0.001$ versus T4; one-way ANOVA, Tukey's test). In fact, aligned filopodia (less than or equal to 15° versus GR) corresponded to 42.9 ± 6.4% and 41 ± 10.5% of the total filopodia emerging from GCs on T2 and T4, respectively. On FLAT, this percentage reduced to 19.6 ± 8.5% ($p < 0.01$ FLAT versus T2 and $p < 0.001$ versus T4; one-way ANOVA, Tukey's test; figure 4*d*). The average angle of the filopodia was 32.1 ± 26.3° and 32 ± 26.9° for T2 and T4, respectively, while on FLAT they showed a random spatial distribution (average angle = 44.6 ± 25.4°; $p < 0.001$ FLAT versus T2 and T4; one-way ANOVA, Kruskal–Wallis test; figure 4*e*), suggesting that both the GRs could similarly interfere with the filopodium development. Finally, our analysis reveals an increase in the F-actin content of the aligned filopodia with respect to the not-aligned ones for both T2 and T4. This actin enrichment was significantly greater than that measured for FLAT ($p < 0.05$ FLAT versus T2 and $p < 0.01$ versus T4; one-way ANOVA, Tukey's test). Finally, we found that aligned filopodia were longer than the perpendicular ones for both T2 and T4 (figure 4*g*), while no difference was measured for FLAT.

Taken together these data demonstrate that leech neurons can effectively read GR topographies and that their tubulin cytoskeleton polarizes along the GR direction. Moreover, leech neurite contact guidance was more efficient on T4 tracks than on T2 tracks. We speculate that the topography-reading process was mediated by filopodium sensing: information from the aligned (longer and richer in actin) and not-aligned (shorted and less rich in actin) filopodia was integrated at the GC level and favoured neurite extension along GR tracks, on both T2 and T4 patterns.

As the capability to drive neurite outgrowth was shown to be dependent on both the dimensions of the underlying pattern and cell type, the response of other, more complex,

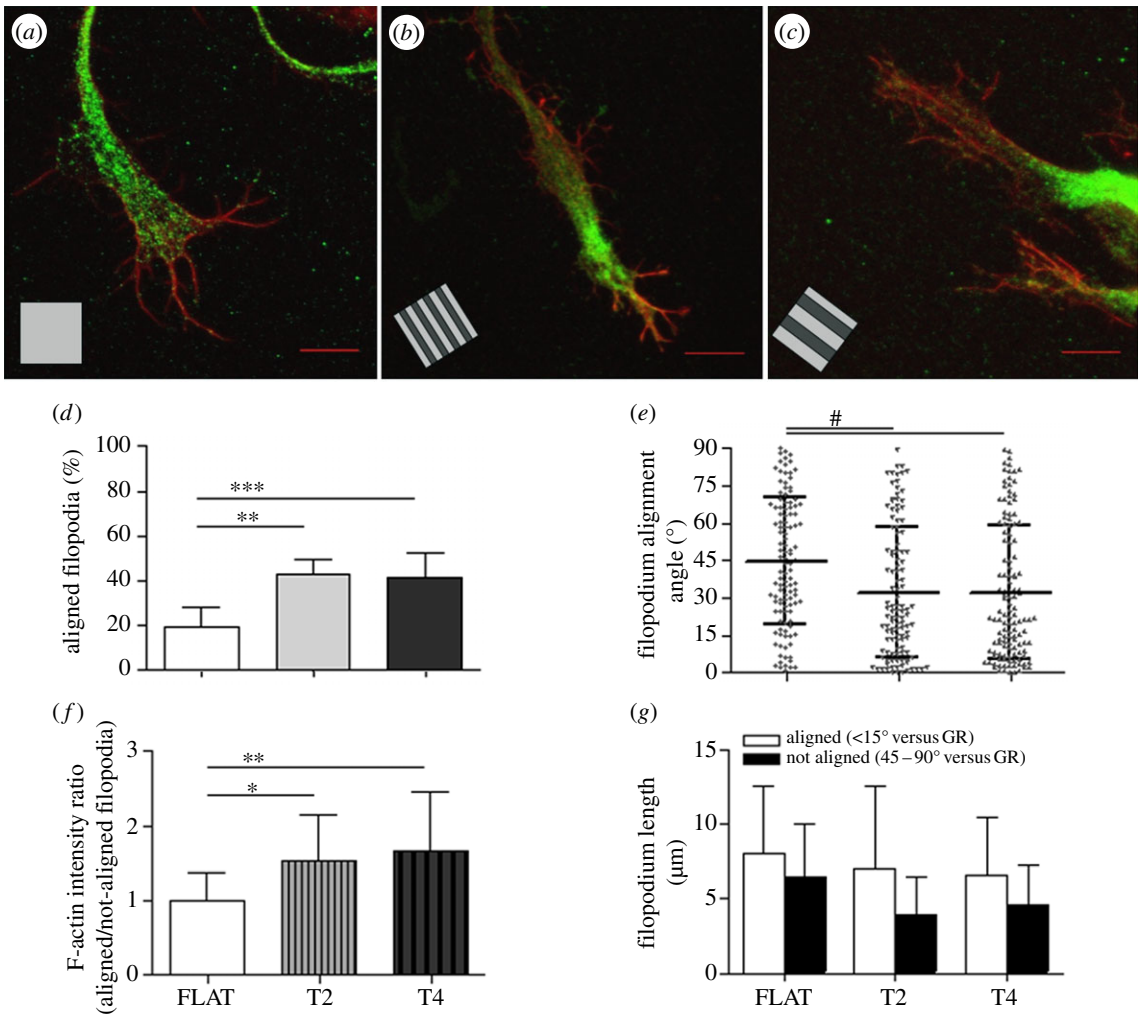

Figure 4. (a–c) High-resolution confocal images of filopodia, immunostained for actin (red), at the GCs of neurites on FLAT (*a*), T2 (*b*) and T4 (*c*); scale bars, 10 μm. (*d–g*) Filopodia at the GCs were traced and analysed: (*d*) percentage of aligned filopodia to the GR (alignment angle less than or equal to 15°); (*e*) mean filopodium alignment angle for the different substrates; (*f*) F-actin intensity in filopodia is reported as the ratio of the actin signal in aligned/not-aligned filopodia; (*g*) mean length of filopodia at GCs, divided into alignment categories. (*d–f*) $*p < 0.05$, $**p < 0.01$, $***p < 0.001$, one-way ANOVA, Tukey's test; (*e*) $\#p < 0.001$, one-way ANOVA, Kruskal–Wallis test. Data are reported as mean ± s.d.

neuronal models to the same nanostructured surfaces was qualitatively investigated to validate the leech neuronal model (figure 5*a*). Confocal images of the cytoskeleton organization (mainly tubulin and actin) of different neuronal cell types on GRs with different periodicity are reported in figure 5. Here, the change in cytoskeleton polarization is evident and present for all the cell types reported. PC12 cells (figure 5*d*) acquired a bipolar morphology aligned to the GR (1-μm-period GR in this case), with an average neurite alignment angle as low as 3.5 ± 0.7° [30]. Also the F11 hybridoma cell line (figure 5*c*), a functional dorsal root ganglion neuronal model, similarly polarized along the GR lines. Moving to a human model, the SH-SY5Y neuroblastoma line (figure 5*b*) differentiated by retinoic acid and BDNF (see §2.2) could mature into a fully developed network on GRs, which resulted in alignment to the underlying lines both for 1- and 2-μm-period GRs [49]. Mouse embryonic stem cells (figure 5*e*) were cultured for two weeks to achieve well-developed network formation and differentiated into neurons: the resulting neuronal tubulin structures on GRs were thick and polarized, reflecting the underlying topography. Finally, we tested primary hippocampal murine neurons, obtaining similar results [49] (figure 5*f*). On flat substrates, all these neuronal cells showed no neurite preferential outgrowth direction and cell shapes were often multipolar (e.g. for PC12, SH-SY5Y) instead of bipolar.

Overall, these data demonstrate that GRs effectively support and tune neurite outgrowth for many neuronal cells. In particular, invertebrate leech neurons showed good neurite contact guidance capabilities (mediated by filopodia) that were retained in vertebrate and human neuronal cell models, suggesting leech neurons as an accessible and proper cell model to study neuronal mechanotransduction.

4. Discussion

By exploiting nanoimprint lithography, we fabricated biocompatible plastic GRs of varying periodicity suitable for high-resolution microscopy and investigated neurite contact guidance of an invertebrate neuronal model (leech neurons). Using high-resolution fluorescence microscopy, we quantitatively compared the changes in tubulin cytoskeleton organization and cell morphology induced by mechanotransduction. The neuritic development and filopodium organization at the GCs were also studied in response to topographical guidance. This

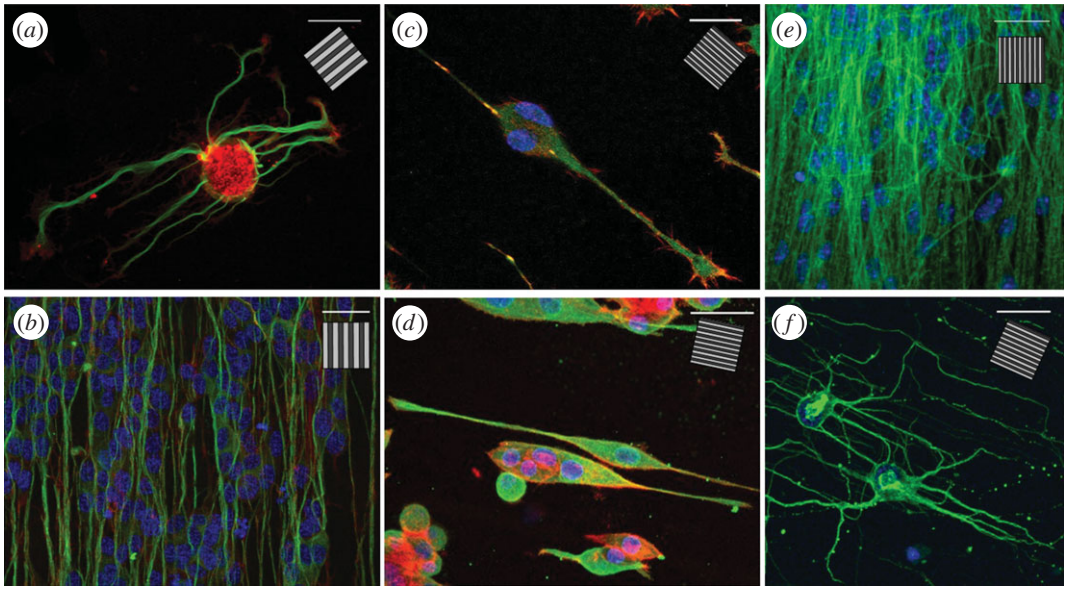

Figure 5. Confocal images of different neuronal cells cultured on GRs. (*a*) A leech neuron grown on T2 and immunostained for tubulin-α (green) and actin (red). (*b*) SH-SY5Y differentiated cells on T2 and immunostained for tubulin-βIII (green) and actin (red). (*c–f*) Smaller neuronal model grown on 1-μm-period GR (0.5 μm linewidth): (*c*) F11 cells immunostained for vinculin (green) and actin (red); (*d*) PC12 cells immunostained for tubulin-βIII (green) and actin (red); (*e*) mouse embryonic stem cells differentiated in neurons and immunostained for tubulin-βIII (green); (*f*) murine hippocampal neurons (D14) immunostained for tubulin-α (green). All samples have been stained with DAPI to visualize nuclei (blue). Scale bars, 30 μm; inset, GR direction.

in vitro model was finally compared and validated with several other neuronal cells, from embryonic stem cells and primary hippocampal neurons to human neuroblastoma differentiated cells, which were interfaced with similar GRs.

Leech neurons could read the directional topographical information of T2 and T4. In particular, cell and neurite network alignment was more efficient on T4 than on T2 and neuron morphology was less branched, in agreement with [44]. The GCs were more streamlined than on FLAT and we observed less filopodium spreading on both T2 and T4. Our data suggest that leech neuron contact guidance is mediated by filopodia sensing. Indeed, aligned filopodia were longer and richer in F-actin, a condition that may favour neurite growth in that direction [19].

It is well known that the morpho-functional response to topographical features can be influenced by neuronal cell type, origin and chemical stimulation, both *in vivo* and *in vitro* [21,52]. For example, it has been recently demonstrated that substrate reading is downstream of the activation of the NGF-induced neuronal differentiation pathway in PC12 cells [30] and that mechanotransduction is enhanced in SY-SY5Y human neuroblastoma cells if treated with retinoic acid and BDNF [49]. Unexpectedly, Rajnicek & McCaig [32] found that embryonic *Xenopus* spinal and rat embryonic hippocampal neurons behave very differently on the same quartz grooves (period 2–8 μm and depth 0.1–1.1 μm): the former grew parallel to the grooves, while the rat neurons displayed a more complex response, growing parallel to wide and deep grooves and perpendicular to the shallow and narrow ones. These aspects have not yet been deeply investigated by the research community, although controlled modulation of mechanotransduction has a clear and profound impact on the design of scaffolds to promote efficient neuronal regeneration.

Our data show that GRs induced qualitatively similar effects on neurite cytoskeleton organization and network development in several different neuronal models, including leech neurons. Interestingly, other than the intrinsic substrate characteristics (e.g. stiffness, nanopattern geometry and aspect ratio), cell morphometric parameters might importantly affect the cell–substrate interaction dynamics and the final neuronal phenotype resulting from this interaction. Leech neurons are large cells (cell body diameter approx. 30 μm) and we measured the best alignment on 4-μm-period GRs (2 μm linewidth). Conversely, small neuronal cell models, such as PC12 or SH-SY5Y (cell body diameter approx. 10 μm), followed 500 nm ridges more efficiently than larger features [31,49]. Overall, larger neuronal cells seem to respond better to larger GR periodicity. These experiments are in agreement with the idea that the actual intensity of the topographical stimulus delivered to cells by contact interaction is not determined by the substrate alone, but it is also dependent on the cell morphological characteristics [46].

As neuronal mechanisms are often conserved during evolution, invertebrate models were often successfully used in neurobiology to help in the understanding of important molecular pathways [37,39,53]. Neuronal contact sensing and mechanotransduction on GRs were conserved among the neuronal types tested here, from invertebrate leech neurons and hybridoma F11 cells to primary hippocampal neurons and a human neuroblastoma model. All together these data suggest that neurite topographical reading might be a conserved mechanism in cells.

Another advantage of the leech model is that neurons can be singularly extracted and cultured *in vitro* [40], whereas in other primary neuronal models the cell concentration is often a critical issue (too few cells can impair culture survival while too many cells can interfere with each other in the development of the neurite network). Furthermore, the size of GCs formed by leech neurons allowed us to identify mechanosensitive cation channels and to characterize their pharmacological properties as well as their modulation, at a single-channel level [41]. These channels show a multi-modal activation, a property typical of transient receptor potential vertebrate channels, whose involvement in axon regeneration has been firmly established [54]. Gentamicin, which is capable of blocking single mechanosensitive channels of leech neurons, enhances their neurite

outgrowth in culture [42]. This result has been confirmed in *Xenopus* neurons [43], suggesting a general role of mechanotransduction in the axon navigation. Accordingly, the findings presented here open up the possibility of investigating the role of the mechanosensitive cation channels in the response of leech neurons to GRs, analysing the effects of treatments aimed at enhancing or depressing the activity of these molecular transducers.

In conclusion, we have reported and characterized neurite contact guidance in leech neurons showing that, similar to other mammalian neuronal models, neurites can align to the substrate main direction. We have shown that this process is mediated by an anisotropic filopodium organization at the GC level. These kinds of topographies are promising for tissue engineering applications, in particular as supporting scaffolds for improving peripheral nerve regeneration after injury. The production of effective tissue-regenerating implants would certainly benefit from a rational design approach, which requires a deep understanding of the molecular mechanisms regulating neuronal and glial interaction with the local physical properties of the extracellular environment. Thus, we feel that increasing effort should be made in this direction instead of relying on a *trial and error* approach. Moreover, further insight into neurite guidance mechanisms will improve our understanding of nervous system development and plasticity and might help to identify novel molecular pathways affected by neurological disorders [3,55].

Funding statement. This work was supported in part by the European Union Seventh Framework Programme (FP7/2007–2013) under grant agreement no. NMP4-LA-2009-229289 NanoII and grant agreement no. NMP3-SL-2009-229294 NanoCARD. This work was also supported by the Regione Toscana through the projects NanoART.

References

1. Ingber DE. 2006 Mechanical control of tissue morphogenesis during embryological development. *Pathology* **266**, 255–266.
2. Arimura N, Kaibuchi K. 2007 Neuronal polarity: from extracellular signals to intracellular mechanisms. *Nat. Rev. Neurosci.* **8**, 194–205. (doi:10.1038/nrn2056)
3. Monje FJ, Kim EJ, Pollak DD, Cabatic M, Li L, Baston A, Lubec G. 2011 Focal adhesion kinase regulates neuronal growth, synaptic plasticity and hippocampus-dependent spatial learning and memory. *Neurosignals* **23**, 1–14.
4. Théry M, Racine V, Piel M, Pépin A, Dimitrov A, Chen Y, Sibarita JB, Bornens M. 2006 Anisotropy of cell adhesive microenvironment governs cell internal organization and orientation of polarity. *Proc. Natl Acad. Sci. USA* **103**, 19 771–19 776. (doi:10.1073/pnas.0609267103)
5. Martínez E, Engel E, Planell J, Samitier J. 2009 Effects of artificial micro- and nano-structured surfaces on cell behaviour. *Ann. Anat.* **191**, 126–135. (doi:10.1016/j.aanat.2008.05.006)
6. Di Rienzo C, Jacchetti E, Cardarelli F, Bizzarri R, Beltram F, Cecchini M. 2013 Unveiling LOX-1 receptor interplay with nanotopography: mechanotransduction and atherosclerosis onset. *Sci. Rep.* **3**, 1141. (doi:10.1038/srep01141)
7. Charron F, Tessier-Lavigne M. 2005 Novel brain wiring functions for classical morphogens: a role as graded positional cues in axon guidance. *Development* **132**, 2251–2262. (doi:10.1242/dev.01830)
8. Woo S, Rowan DJ, Gomez TM. 2009 Retinotopic mapping requires focal adhesion kinase-mediated regulation of growth cone adhesion. *J. Neurosci.* **29**, 13 981–13 991. (doi:10.1523/JNEUROSCI.4028–09.2009)
9. Myers JP, Gomez TM. 2011 Focal adhesion kinase promotes integrin adhesion dynamics necessary for chemotropic turning of nerve growth cones. *J. Neurosci.* **31**, 13 585–13 595. (doi:10.1523/JNEUROSCI.2381–11.2011)
10. Yokota Y, Gashghaei HT, Han C, Watson H, Campbell KJ, Anton ES. 2007 Radial glial dependent and independent dynamics of interneuronal migration in the developing cerebral cortex. *PLoS ONE* **2**, e794. (doi:10.1371/journal.pone.0000794)
11. Yoshimura T, Arimura N, Kaibuchi K. 2006 Signaling networks in neuronal polarization. *J. Neurosci.* **26**, 10 626–10 630. (doi:10.1523/JNEUROSCI.3824-06.2006)
12. Gomez N, Chen S, Schmidt CE. 2007 Polarization of hippocampal neurons with competitive surface stimuli: contact guidance cues are preferred over chemical ligands. *J. R. Soc. Interface* **4**, 223–233. (doi:10.1098/rsif.2006.0171)
13. Vitriol EA, Zheng JQ. 2012 Growth cone travel in space and time: the cellular ensemble of cytoskeleton, adhesion, and membrane. *Neuron* **73**, 1068–1081. (doi:10.1016/j.neuron.2012.03.005)
14. Johansson F, Carlberg P, Danielsen N, Montelius L, Kanje M. 2006 Axonal outgrowth on nano-imprinted patterns. *Biomaterials* **27**, 1251–1258. (doi:10.1016/j.biomaterials.2005.07.047)
15. Meyer G, Feldman EL. 2002 Signaling mechanisms that regulate actin-based motility processes in the nervous system. *J. Neurochem.* **83**, 490–503. (doi:10.1046/j.1471-4159.2002.01185.x)
16. Dityatev A, Rusakov D. 2011 Molecular signals of plasticity at the tetrapartite synapse. *Curr. Opin. Neurobiol.* **21**, 353–359. (doi:10.1016/j.conb.2010.12.006)
17. Woo S, Gomez TM. 2006 Rac1 and RhoA promote neurite outgrowth through formation and stabilization of growth cone point contacts. *J. Neurosci.* **26**, 1418–1428. (doi:10.1523/JNEUROSCI.4209-05.2006)
18. Geiger B, Spatz JP, Bershadsky AD. 2009 Environmental sensing through focal adhesions. *Nat. Rev. Mol. Cell Biol.* **10**, 21–33. (doi:10.1038/nrm2593)
19. Jang KJ, Kim MS, Feltrin D, Jeon NL, Suh KY, Pertz O. 2010 Two distinct filopodia populations at the growth cone allow to sense nanotopographical extracellular matrix cues to guide neurite outgrowth. *PLoS ONE* **5**, e15966. (doi:10.1371/journal.pone.0015966)
20. Sergi PN, Morana Roccasalvo I, Tonazzini I, Cecchini M, Micera S. 2013 Cell guidance on nanogratings: a computational model of the interplay between pc12 growth cones and nanostructures. *PLoS ONE*. **8**, e70304. (doi:10.1371/journal.pone.0070304)
21. Valiente M, Ciceri G, Rico B, Marín O. 2011 Focal adhesion kinase modulates radial glia-dependent neuronal migration through connexin-26. *J. Neurosci.* **31**, 11 678–11 691. (doi:10.1523/JNEUROSCI.2678–11.2011)
22. Di Cristo G, Chattopadhyaya B, Kuhlman SJ, Fu Y, Bélanger MC, Wu CZ, Rutishauser U, Maffei L, Huang ZJ. 2007 Activity-dependent PSA expression regulates inhibitory maturation and onset of critical period plasticity. *Nat. Neurosci.* **10**, 1569–1577. (doi:10.1038/nn2008)
23. Eshghi S, Schaffer DV. 2008 *Engineering microenvironments to control stem cell fate and function.* StemBook 1–12. Cambridge, MA: Harvard Stem Cell Institute. (doi:10.3824/stembook.1.5.1)
24. Wieringa P, Tonazzini I, Micera S, Cecchini M. 2012 Nanotopography induced contact guidance of the F11 cell line during neuronal differentiation: a neuronal model cell line for tissue scaffold development. *Nanotechnology* **23**, 275102. (doi:10.1088/0957-4484/23/27/275102)
25. Tonazzini I *et al*. 2010 Multiscale morphology of organic semiconductor thin films controls the adhesion and viability of human neural cells. *Biophys. J.* **98**, 2804–2812. (doi:10.1016/j.bpj.2010.03.036)
26. Valle F, Chelli B, Bianchi M, Greco P, Bystrenova E, Tonazzini I, Biscarini F. 2010 Stable non-covalent large area patterning of inert teflon-AF surface: a new approach to multiscale cell guidance. *Adv. Eng. Mat.* **12**, B185–B191. (doi:10.1002/adem.201080022)
27. Tonazzini I, Meucci S, Faraci P, Beltram F, Cecchini M. 2013 Neuronal differentiation on anisotropic substrates

and the influence of nanotopographical noise on neurite contact guidance. *Biomaterials* **34**, 6027–6036. (doi:10.1016/j.biomaterials.2013.04.039)

28. Kim YT, Haftel VK, Kumar S, Bellamkonda RV. 2008 The role of aligned polymer fiber-based constructs in the bridging of long peripheral nerve gaps. *Biomaterials* **29**, 3117–3127. (doi:10.1016/j.biomaterials.2008.03.042)
29. Ferrari A, Cecchini M, Serresi M, Faraci P, Pisignano D, Beltram F. 2010 Neuronal polarity selection by topography-induced focal adhesion control. *Biomaterials* **31**, 4682–4694. (doi:10.1016/j.biomaterials.2010.02.032)
30. Ferrari A, Faraci P, Cecchini M, Beltram F. 2010 The effect of alternative neuronal differentiation pathways on PC12 cell adhesion and neurite alignment to nanogratings. *Biomaterials* **31**, 2565–2573. (doi:10.1016/j.biomaterials.2009.12.010)
31. Ferrari A, Cecchini M, Dhawan A, Micera S, Tonazzini I, Stabile R, Pisignano D, Beltram F. 2011 Nanotopographic control of neuronal polarity. *Nano Lett.* **11**, 505–511. (doi:10.1021/nl103349s)
32. Rajnicek A, McCaig C. 1997 Guidance of CNS growth cones by substratum grooves and ridges: effects of inhibitors of the cytoskeleton, calcium channels and signal transduction pathways. *J. Cell Sci.* **110**, 2915–2924.
33. Franco D *et al*. 2013 Accelerated endothelial wound healing on microstructured substrates under flow. *Biomaterials* **34**, 1488–1497. (doi:10.1016/j.biomaterials.2012.10.007)
34. Acklin SE, Nicholls JG. 1990 Intrinsic patterns and extrinsic factors influencing properties of identified leech neurons in culture growth. *J. Neurosci.* **10**, 1082–1090.
35. Neely MD, Macaluso E. 1997 Motile areas of leech neurites are rich in microfilaments and two actin-binding proteins: gelsolin and profilin. *Proc. R. Soc. B* **264**, 1701–1706. (doi:10.1098/rspb.1997.0236)
36. Pellegrino M, Orsini P, De Gregorio F. 2009 Use of scanning ion conductance microscopy to guide and redirect neuronal growth cones. *Neurosci. Res.* **64**, 290–296. (doi:10.1016/j.neures.2009.03.014)
37. Ayali A. 2012 Editorial: models of invertebrate neurons in culture. *J. Mol. Histol.* **43**, 379–381. (doi:10.1007/s10735-012-9416-0)
38. Fernandez-de-Miguel F, Drapeau P. 1995 Synapse formation and function: insights from identified leech neurons in culture. *J. Neurobiol.* **27**, 367–379. (doi:10.1002/neu.480270309)
39. Giachello CNG, Montarolo PG, Ghirardi M. 2012 Synaptic functions of invertebrate varicosities: what molecular mechanisms lie beneath. *Neural Plast.* **2012**, 670821. (doi:10.1155/2012/670821)
40. Schmold N, Syed NI. 2012 Molluscan neurons in culture: shedding light on synapse formation and plasticity. *J. Mol. Histol.* **43**, 383–899. (doi:10.1007/s10735–012–9398-y)
41. Pellegrino M, Pellegrini M. 2007 Mechanosensitive channels in neurite outgrowth. *Curr. Top. Membr.* **59B**, 111–125. (doi:10.1016/S1063-5823(06)59005-2)
42. Calabrese B, Manzi S, Pellegrini M, Pellegrino M. 1999 Stretch-activated cation channels of leech neurons: characterization and role in neurite outgrowth. *Eur. J. Neurosci.* **11**, 2275–2284. (doi:10.1046/j.1460-9568.1999.00648.x)
43. Jacques-Fricke BT, Seow Y, Gottlieb PA, Sachs F, Gomez T. 2006 Ca^{2+} influx through mechanosensitive channels inhibits neurite outgrowth in opposition to other influx pathways and release from intracellular stores. *J. Neurosci.* **26**, 5656–5664. (doi:10.1523/JNEUROSCI.0675-06.2006)
44. Baranes K, Kollmar D, Chejanovsky N, Sharoni A, Shefi O. 2012 Interactions of neurons with topographic nano cues affect branching morphology mimicking neuron–neuron interactions. *J. Mol. Hist.* **43**, 437–447. (doi:10.1007/s10735-012-9422-2)
45. Baranes K, Chejanovsky N, Alon N, Sharoni A, Shefi O. 2012 Topographic cues of nano-scale height direct neuronal growth pattern. *Biotechnol. Bioeng.* **109**, 1791–1797. (doi:10.1002/bit.24444)
46. Meucci S, Tonazzini I, Beltram F, Cecchini M. 2012 Biocompatible noisy nanotopographies with specific directionality for controlled anisotropic cell cultures. *Soft Matter* **8**, 1109–1119. (doi:10.1039/c1sm06256e)
47. Chiquet M, Acklin SE. 1986 Attachment of Con A or extracellular matrix initiates rapid sprouting by cultured leech neurons. *Proc. Natl Acad. Sci. USA* **83**, 6188–6192. (doi:10.1073/pnas.83.16.6188)
48. Borgesius NZ, Woerden GM, Van Buitendijk GHS, Keijzer N, Jaarsma D, Hoogenraad CC, Elgersma Y. 2011 BCaMKII plays a nonenzymatic role in hippocampal synaptic plasticity and learning by targeting aCaMKII to synapses. *J. Neurosci.* **31**, 10 141–10 148. (doi:10.1523/JNEUROSCI.5105-10.2011)
49. Tonazzini I, Cecchini A, Elgersma Y, Cecchini M. 2013 Interaction of SH-SY5Y cells with nanogratings during neuronal differentiation: comparison with primary neurons. *Adv. Healthc. Mater*. (doi:10.1002/adhm.201300216)
50. Fico A, Manganelli G, Simeone M, Guido S, Minchiotti G, Filosa S. 2008 High-throughput screening-compatible single-step protocol to differentiate embryonic stem cells in neurons. *Stem Cells Dev.* **17**, 573–584. (doi:10.1089/scd.2007.0130)
51. Juraska JM. 1982 The development of pyramidal neurons after eye opening in the visual cortex of hooded rats: a quantitative study. *Comp. Neurol.* **212**, 208–213. (doi:10.1002/cne.902120210)
52. Smeal RM, Tresco P. 2008 The influence of substrate curvature on neurite outgrowth is cell type dependent. *Exp. Neurol.* **213**, 281–292. (doi:10.1016/j.expneurol.2008.05.026)
53. Nicholls JG. 1987 The search for connections: studies of regeneration in the nervous system of the leech. *Magnes. Lecture Set.* **2**, 1–86.
54. Kerstein PC, Jacques-Fricke BT, Rengifo J, Mogen BJ, Williams JC, Gottlieb PA, Sachs F, Gomez TM. 2013 Mechanosensitive TRPC1 channels promote calpain proteolysis of talin to regulate spinal axon outgrowth. *J. Neurosci.* **33**, 273–285. (doi:10.1523/JNEUROSCI.2142-12.2013)
55. Jaalouk DE, Lammerding J. 2009 Mechanotransduction gone awry. *Nat. Rev. Mol. Cell Biol.* **10**, 63–73. (doi:10.1038/nrm2597)